AIAA JOURNAL
Vol. 43, No. 1, January 2005

Modeling the Buckling of Axially Compressed Elastic Cylindrical Shells

S. R. Bodner* and M. B. Rubin†
Technion—Israel Institute of Technology, 32000 Haifa, Israel

This exercise is intended to provide a direct correlation between the axial compressive buckling of elastic thin-walled cylinders and the response of a mechanical model that exhibits a peak load at large deformation. The model is similar, but more general, to those used by Budiansky and Hutchinson and by Kounadis and associates to illustrate dynamic buckling behavior of imperfection sensitive nonlinear systems. Here, an empirical relation between observed static shell buckling loads and the shell geometry is used to characterize the restraining spring parameter of the model. The resulting model indicates realistic imperfection sensitivity of the load-deflection relation and, as a good physical analogy, provides insight into the shell buckling mechanism. Specifically, from the perspective of the model, shell buckling is viewed as a local event governed by shallow arch-like behavior where the extent of the arch depends on the shell geometry. This implies that the specific geometry of local axial imperfections of the shell (out of straightness) might be more important than that of circumferential imperfections (out of roundness) for shell buckling under axial loading. Moreover, use of an imperfection slope factor rather than an imperfection displacement term might be more suitable for actual shells in some cases. In addition, the model analogy indicates that the buckling (peak) load also depends on the shell geometry and that the bifurcation load serves only as a reference value. A comparison is made to Koiter's approximate formula for axially compressed isotropic shells.

Introduction

DESPITE the enormous attention that has been given to the problem of the buckling of thin-walled elastic cylindrical shells under axial compression, there is still some uncertainty with the proposed treatments. This is evidenced by the occasional notes and comments on the subject that still appear in the literature. One of the reasons is that the main features of geometric imperfections that influence postbuckling response have not been fully identified. Recent approaches to buckling load calculations include high-fidelity-analyses that emphasize the need for sophisticated numerical methods and an international data bank of shell imperfections.[1,2]

The essential difficulty of the problem is the extensive postbuckling reduction in equilibrium load from the bifurcation condition, which is thereby an unstable state. This is caused primarily by the development of tensile membrane stresses caused by stretching in the buckling mode. For plates that experience similar effects, the applied compressive load is carried without reduction by the boundary regions near fixed supports. In the case of hydrostatically loaded cylindrical shells, the additional compressive circumferential stress negates the tendency for full unloading. Experimental observations on elastic cylindrical shells under axial compression, as summarized by Singer et al.,[3,4] indicate that the onset of buckling is highly localized over a small region of the structure. Subsequently, the buckling deformation expands to develop a diamond-shaped pattern that is repeated in neighboring sections that can cover most of the shell surface. A consequence of the initial localized buckling is that the remaining intact specimen acts as a soft spring so that the loading at the initiation of buckling is essentially one of constant force. However, as the buckle pattern develops and spreads, the load drops at fixed overall displacement. A simplistic view of the diamond-shaped buckle pattern is that it resembles a buckled axial strip supported at its middle by a flexible foundation, which exhibits snap through caused by shallow arch-like behavior in the circumferential direction.

The present paper is a further examination of the problem through an analysis of a modified version of a previously used mechanical model that exhibits some of the buckling characteristics of the axially compressed cylindrical shell. The intention is to correlate the response of the model to loading with observations of the shell buckling process. For the mechanical model with an initial imperfection, the full nonlinear load-deflection relation is determined from the onset of loading. Moreover, as observed in the shell response, the buckling (peak) load of the model is sensitive to imperfections and can be substantially lower than its bifurcation load. This exercise is intended to contribute to physical understanding of the shell buckling process, which can be helpful in directing further analytical and computational investigations.

Background

The problem of postbifurcation reduction of the equilibrium load for certain classes of elastic shells and loading conditions was addressed by von Kármán and associates in the early 1940s. They postulated the existence of a lower bound on the buckling load caused by the presence of modest initial geometrical imperfections of the shell. This lower-bound assumption (the minimum of the load-deflection relation for a perfect shell) was subsequently shown by Friedrichs[5] to be not rigorous from the mathematical viewpoint. With subsequent studies, it was recognized that the essential problem was the determination of the peak (buckling) load of an imperfect structure in the large deformation range. The work of Koiter[6] was an important contribution to the subject.

Hutchinson and Koiter[7] discussed the general postbifurcation behavior of elastic structures from the perspective of the original work of Koiter, which emphasized the importance of sensitivity to geometric imperfections for certain conditions. Depending on the type of structure and the type of loading, the postbifurcation response can be characterized by an increasing load (such as that experienced by elastic columns or in-plane compressed elastic plates that are supported by fixed edges) or by a decreasing load leading to unstable behavior such as that in an axially compressed circular cylindrical shell. These latter structures and loadings exhibit imperfection sensitive response because the peak static load P_s, which can be supported by the structure, is sensitive to geometric imperfections.

Received 15 February 2004; revision received 22 June 2004; accepted for publication 29 June 2004.

*Professor Emeritus, Faculty of Mechanical Engineering.
†Professor, Faculty of Mechanical Engineering.

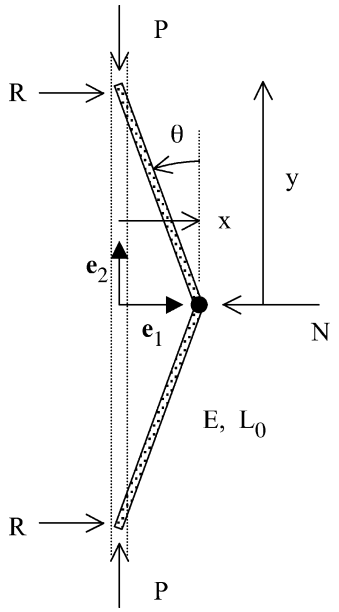

Fig. 1 Sketch of the buckling model.

Specifically, for axially compressed cylindrical shells Koiter's work leads to an approximate formula for the case of axisymmetric buckling with axisymmetric imperfections of the form [Ref. 7, Eq. (7)]

$$(1-\sigma_s/\sigma_c)^2 = \left[3\sqrt{3(1-\nu^2)}\Big/2\right](\sigma_s/\sigma_c)\psi \tag{1}$$

In Eq.(1) σ_c is the classical value of the axial stress at bifurcation (e.g., Timoshenko and Gere[8])

$$\sigma_c/E = \kappa\Big/\sqrt{3(1-\nu^2)} \tag{2}$$

where E is Young's modulus, ν is Poisson's ratio, κ is the ratio of the thickness t to the radius R of the shell,

$$\kappa = t/R \tag{3}$$

σ_s is the value of axial stress at the peak load, and ψ is the geometric imperfection amplitude δ divided by the shell thickness. Such an approximate analytical solution for a continuous system is based on introducing specific modes that reduce the number of degrees of freedom. In this sense, it is somewhat similar to introducing a simple finite degree-of-freedom mechanical model of the physical phenomena.

In a series of papers, Budiansky and Hutchinson,[9] Budiansky,[10] and Hutchinson and Budiansky[11] analyzed dynamic buckling of elastic structures following Koiter's formulation for the case of imperfection sensitivity. Figure 1 shows a modified version of a simple mechanical model introduced in these papers for single-mode analysis of dynamic buckling. In their model, the bars were taken to be rigid of length L_0, a mass was introduced at the hinge, and the trigonometric functions in the resulting formulas were approximated up to second order. When the restoring force N in Fig. 1 is represented by a quadratic softening spring, the peak static load P_s is given by [Ref. 10, Eq. (24)]

$$(1-P_s/P_c)^2 = 4(-a)(P_s/P_c)\psi, \qquad P_c = A\sigma_c, \qquad P_s = A\sigma_s \tag{4}$$

Here, A is the reference cross-sectional area of the shell, the normalized geometric imperfection parameter $\bar{\xi}$ in Ref. 10, Eq. (24), has been replaced by ψ, and $(-a)$ is a positive number characterizing the magnitude of the softening of the quadratic spring. Comparison of Eq. (1) with Eq. (4) reveals that the simple mechanical model captures the main features of the peak static load of a geometrically imperfect axially compressed cylindrical shell. A similar model has been used more recently by Kounadis et al.[12] for further studies on dynamic buckling.

Koiter's formula [Eq. (1)] predicts that the ratio σ_s/σ_c for a circular cylindrical shell depends only on Poisson's ratio and on the imperfection parameter ψ. For this reason, numerous papers have been focused on defining and measuring this geometric imperfection parameter.

With regard to actual buckling loads of axially compressed shells, von Kármán et al.[13] [Eq. (13) and Fig. 14] plotted the peak stress in quasi-static experiments and concluded that an empirical fit leads to the form

$$\sigma_s/\sigma_c = \text{constant} \times \kappa^{0.4} \tag{5}$$

More recently, Calladine[14] proposed a similar empirical formula for σ_s based on additional test results, which, in view of Eq. (2), yield

$$\sigma_s/\sigma_c = 5\sqrt{3(1-\nu^2)}\,\kappa^{\frac{1}{2}} = 8.3\kappa^{\frac{1}{2}} \qquad \text{for} \qquad \nu = 0.3 \tag{6}$$

For the remainder of this paper, the empirical formula (6) will be used.

One possible method of reconciling the theoretical result (1) with the empirical formula (6) is to assume that ψ depends on κ. Specifically, substituting Eq. (6) into Eq. (1) yields

$$\psi = \left[\frac{2}{45(1-\nu^2)}\right]\frac{\left[1-5\sqrt{3(1-\nu^2)}\,\kappa^{\frac{1}{2}}\right]^2}{\kappa^{\frac{1}{2}}} \tag{7}$$

but this eliminates the possibility of predicting the sensitivity of the peak load to different measured geometric imperfections. Hoff[15] suggested that ψ in Koiter's work, Eq. (1), could be expressed as a function of κ for expertly made, well-made, and ordinary shells, but this leads to the same difficulty.

Another possibility of reconciling theory with empirical data is suggested by the formula (4) associated with the single-mode mechanical model. Specifically, this formula shows that the ratio P_s/P_c depends not only on the imperfection parameter ψ, but it also depends on the parameter $(-a)$. Although Hutchinson and Koiter[7] [see α in Eq. (2)] mentioned that $(-a)$ depends on properties of the structure, quantification of this dependence was not pursued. In the following analysis of the modified model sketched in Fig. 1, it is shown that the equations lead to an approximate formula of the form

$$(1-P_s/P_c)^2 = \tfrac{8}{3}[1-P_c/(E_bA_b)](P_s/P_c)(\theta_0/\beta) \tag{8}$$

where E_b is Young's modulus of each bar, A_b is the cross-sectional area of each bar, θ_0 is an angular measure of geometric imperfection, and β relates to the spring force N.

The approach of the present paper is to correlate the behavior of the mechanical model in Fig. 1 with that of actual axially compressed shells specified by Eq. (6). The consequences of the empirical fitting are then examined with respect to the model's predictive capability.

Modified Mechanical Model

A sketch of the model in a deformed state is shown in Fig. 1. The basic elements are two bars of stress-free length L_0, which are considered here to be elastic in compression and rigid in bending in order to predict more realistic load-deflection response and to allow for the possible transfer of energy in compression to energy in the lateral spring. They are pinned together at one set of ends, and a spring resists their lateral motion at the hinge point by a developed force N. A colinear set of forces P acts at the unpinned ends of the bars, and the end displacements are constrained to the direction of these forces by reaction forces R. In particular, the lateral force N is specified as a nonlinear spring element, which simulates the response of a shallow arch to a central force. This model is reminiscent of the specimens in the tests by von Kármán et al.[13] of an axially loaded column supported by a lateral circular hoop at its center, and, as discussed earlier, is a modified form of the model of Hutchinson and Budiansky.[11] In the following, the model equations are solved exactly without approximating the geometric nonlinearities.

With θ being the inclination angle between the bars and the direction of the force P, equilibrium requires

$$P = P_b \cos\theta \tag{9a}$$

$$R = P_b \sin\theta \tag{9b}$$

$$N = 2P_b \sin\theta \tag{9c}$$

where P_b is the axial compressive force in each bar. That force is related to the bar's deformed length L by

$$P_b/(E_b A_b) = (1 - L/L_0) \tag{10}$$

where the length L is related to the coordinates $\{x, y, \theta\}$ in Fig. 1 by

$$L = \sqrt{x^2 + y^2} \tag{11a}$$

$$x = L \sin\theta \tag{11b}$$

$$y = L \cos\theta \tag{11c}$$

Moreover, the unloaded state is specified by the initial value θ_0, such that

$$x_0/L_0 = \sin(\theta_0), \qquad y_0/L_0 = \cos(\theta_0) \tag{12}$$

The lateral restraining spring is taken to be a nonlinear cubic function of the displacement $(x–x_0)$ from the initial state, which approximately corresponds to the response of a shallow arch to midpoint loading. On that basis, the spring force is given by

$$N(\eta) = (2\alpha\beta/9)(\eta^2 - 6\eta + 9)\eta \tag{13}$$

where the amplitude is divided into two terms: α having the dimension of force, β being non-dimensional, and the numerical terms are chosen for subsequent convenience. In Eq. (13), η is the normalized lateral displacement from the unloaded position x_0 defined by

$$\eta = (x - x_0)/(\beta L_0) = (1/\beta)[(y/L_0)\tan\theta - \sin(\theta_0)] \tag{14}$$

where use has been made of Eqs. (11) and (12) to rewrite the expression for η in terms of y and θ. [Note that Eq. (14) also depends on the quantity β associated with the spring force (13)]. It then follows that

$$\frac{dN}{dx} = \frac{2\alpha}{3L_0}(1 - \eta)(3 - \eta) \tag{15a}$$

$$\frac{dN}{dx}(0) = \frac{2\alpha}{L_0} \tag{15b}$$

$$\frac{dN}{dx}(1) = 0 \tag{15c}$$

$$N(0) = 0 \tag{15d}$$

$$N(1) = \frac{8\alpha\beta}{9} \tag{15e}$$

$$N(3) = 0 \tag{15f}$$

so that the spring force has an initial slope of $(2\alpha/L_0)$ and a peak at $\eta = 1$ of magnitude $(\frac{8}{9})\alpha\beta$. An analysis of the bifurcation condition for the geometrically perfect model $(\theta_0 = 0)$ indicates that the bifurcation load P_c would be $(\frac{1}{2})KL$, where K is the initial spring constant of the restraining spring, so that

$$P_c = \frac{1}{2}KL = \frac{1}{2}\frac{dN}{dx}(0)L = \alpha\frac{L}{L_0} = \alpha\left(1 - \frac{P_c}{E_b A_b}\right) \tag{16}$$

where use has been made of Eq. (9a) with $\theta = 0$ and Eq. (10). Thus, α (the other component of the spring force) is related to the bifurcation load P_c of the perfect model $(\theta_0 = 0)$ by the formula

$$\alpha = P_c/[1 - P_c/(E_b A_b)] \tag{17}$$

which can serve as a reference value. With α fixed, the force in the spring is controlled by the term β.

To solve the equilibrium equations for positive θ, it is convenient to specify a value for η and then solve Eq. (14) for y:

$$\frac{y}{L_0} = \left[\frac{\beta\eta + \sin(\theta_0)}{\tan\theta}\right] \tag{18}$$

With the help of Eqs. (10), (11c), and (18), it follows that

$$\frac{L}{L_0} = \left[\frac{\beta\eta + \sin(\theta_0)}{\sin\theta}\right] \tag{19a}$$

$$\frac{P_b}{E_b A_b} = \left\{1 - \left[\frac{\beta\eta + \sin(\theta_0)}{\sin\theta}\right]\right\} \tag{19b}$$

Next, substituting Eq. (19b) into Eq. (9c) and using Eq. (13) yields an equation for θ of the form

$$\sin\theta = \sin(\theta_0) + \beta\eta + (\beta/9)[\alpha/(E_b A_b)](\eta^2 - 6\eta + 9)\eta \tag{20}$$

Also, the axial deflection δ of the end of each bar and its nondimensional value Δ are defined by

$$\Delta = \delta/L_0 = (y_0 - y)/L_0 \tag{21}$$

It then follows that the main quantities in the model can be summarized in the nondimensional forms

$$\frac{P}{E_b A_b} = \left\{1 - \left[\frac{\beta\eta + \sin(\theta_0)}{\sin\theta}\right]\right\}\cos\theta \tag{22a}$$

$$\frac{N}{E_b A_b} = 2\left\{1 - \left[\frac{\beta\eta + \sin(\theta_0)}{\sin\theta}\right]\right\}\sin\theta \tag{22b}$$

$$\Delta = \cos(\theta_0) - \left[\frac{\beta\eta + \sin(\theta_0)}{\tan\theta}\right] \tag{22c}$$

Thus, for specified values of the nondimensional quantities

$$\{P_c/(E_b A_b), \beta, \theta_0\}$$

it is possible to solve Eq. (20) for θ for any positive value of η and then use Eq. (22) to determine the entire force-deflection curve. Of particular interest is the ratio of the peak load P_s to the bifurcation load P_c. In these equations, α and $P_c/(E_b A_b)$ characterize the bifurcation load, β controls the response of the lateral restraining spring, and θ_0 is the initial geometric imperfection $(\theta_0 > 0)$. By definition, the ratio P_s/P_c is unity for the perfect structure $(\theta_0 = 0)$. For imperfect structures $(\theta_0 > 0)$, it will be seen that this ratio can be much less than unity because the model exhibits significant load reduction sensitivity to imperfections.

Correlation of Mechanical Model with a Cylindrical Shell

The simple mechanical model was developed to illustrate the main observations in the buckling of axially compressed shells. To carry the analogy further and to provide insights into physical details and into proposed analytical formulations of the shell problem, it is useful to correlate the essential parameters of the model with those of the shell. These model parameters consist of 1) the normalized bifurcation load $P_c/(E_b A_b)$ of the geometrically perfect model, which relates to that of the perfect shell; 2) the term β, which characterizes the lateral restraining spring in the model and should therefore be related to a structural parameter of the shell; 3) the term θ_0 in the model, which is analogous to the initial geometric imperfection in the shell structure; and 4) the ratio of the peak load P_s of the load-deflection relation to the bifurcation load P_c in the model, which should be related to that of the shell.

For the case of the respective bifurcation loads, the nondimensional bifurcation stress in the model $P_c/(E_b A_b)$ should correspond to the classical bifurcation stress (2) for the axially compressed shell.

It then follows from Eq. (2) that

$$P_c/(E_bA_b) \rightarrow \sigma_c/E = 0.6\kappa \qquad \text{for} \qquad \nu = 0.3 \qquad (23)$$

Furthermore, the empirical formula (6) for the actual buckling (peak) stress σ_s normalized by the bifurcation stress σ_c suggests the correlation

$$P_s/P_c \rightarrow \sigma_s/\sigma_c = 8.3\kappa^{\frac{1}{2}} \qquad \text{for} \qquad \nu = 0.3 \qquad (24)$$

In general, the ratio P_s/P_c of the model is a function of the three parameters $\{P_c/(E_bA_b), \beta, \theta_0\}$. Once the correlation (23) has been made, the model will produce the same bifurcation load as the shell. Therefore, the model can be further correlated with the shell by adjusting the two parameters β and θ_0 to enforce the condition (24).

Correlation Based on the Spring (Structural) Parameter β

The inference taken here is that β should characterize the shell structure through dependence on the basic geometry κ of the shell. In this approach, the initial geometric imperfection θ_0 is held constant, and the parameter β is proposed as a function of κ. In principle, it is possible for a given θ_0 to determine the function $\beta(\kappa)$, which would cause the solution of the model to enforce the correlation (24) exactly. Specifically, the peak load of the model is a function of $\beta(\kappa)$ and θ_0. However, obtaining a closed-form analytical expression for this function does not seem possible. Instead, an approximate expression for β is developed in the Appendix, which takes the form

$$\beta(\kappa) = \hat{\beta}\left[P_c/(E_bA_b),\, P_s/P_c,\, \theta_0^*\right] \qquad (25)$$

where θ_0^* is a value of θ_0 specified later.

The analysis in the Appendix shows that for small values of θ_0 and (θ_0/β) the approximate equation for P_s/P_c reduces to Eq. (8). The close correspondence between Eqs. (8) and (1) can be seen more clearly for the typical case when $P_c/(E_bA_b)$ is negligible relative to unity [which is equivalent to ignoring the change in the bar's length $(L–L_0)$ prior to bifurcation], so that Eq. (8) becomes

$$(1 - P_s/P_c)^2 = 2.67(P_s/P_c)(\theta_0/\beta) \qquad (26)$$

whereas for $\nu = 0.3$, Eq. (1) becomes

$$[1 - \sigma_s/\sigma_c]^2 = 2.48[\sigma_s/\sigma_c]\psi \qquad (27)$$

The important difference between these equations is that Koiter's form (27) suggests that the buckling (peak) load depends only on a geometric imperfection parameter ψ, whereas Eq. (26) suggests that it depends on both a geometric imperfection θ_0 and a spring parameter β related to the shell's structure. Consequently, in the mechanical model the effect of the lateral restraining spring has an essential influence on the buckling load through the value of β.

Next setting

$$P_c/(E_bA_b) = 0.6\kappa, \qquad P_s/P_c = 8.3\kappa^{\frac{1}{2}} \qquad (28)$$

and choosing

$$\theta_0^* = 1\,\text{deg} = \pi/180 \qquad (29)$$

as a representative small value, it is possible to determine $\beta(\kappa)$, which causes the value of P_s/P_c in the model to be close to the correlation value (24) when the geometric imperfection θ_0 equals the specified value θ_0^*. Once the functional form for β is specified (25), it can be used together with the correlation (23) to determine the nonlinear response of the complete model equations (22) for any value of the geometric imperfection θ_0. Figure 2 shows the values of this function, and Fig. 3 shows the predictions of the peak load in the model using this function and different values of the geometric imperfection θ_0. Also, shown in Fig. 3 is that the peak load of the model for $\theta_0 = \theta_0^*$ is very close to the empirical values (24), which justifies the approximations in the Appendix. Moreover, from Fig. 3 it is seen that the variation of P_s/P_c with $1/\kappa$ would be very close to the NASA-recommended design curve [Ref. 16, Eq. (2)] for θ_0 set to about 1.5 deg.

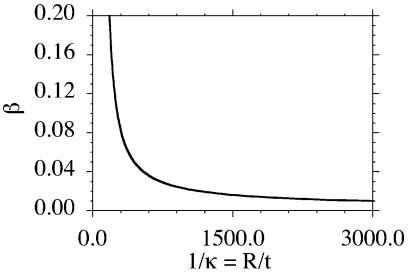

Fig. 2 Values of the spring (structural) parameter $\beta(\kappa)$ given in Eqs. (25) and (A9).

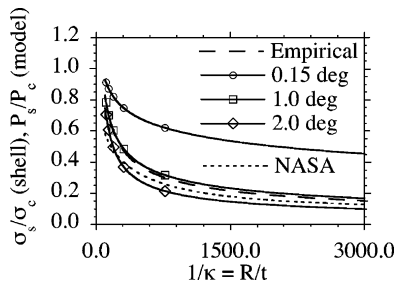

Fig. 3 Values of the peak load predicted by the model for different values of the imperfection angle θ_0 and comparison with the empirical values (6) and the NASA values.

The imperfection parameter θ_0 in the model is not necessarily directly identified with the term ψ commonly used in the analyses of shells because θ_0 could be interpreted in the model as both a slope imperfection and as a displacement imperfection. The determination of the appropriate value of ψ for actual shells has been the subject of extensive investigation. Within the context of the simple model, it is not possible to separate the effects of a displacement imperfection from an angular imperfection. However, use of an imperfection slope factor rather than an imperfection displacement term might be more suitable for actual shells in some cases.

Additional calculations were performed for the detailed response characteristics of the model with $\beta = \beta(\kappa)$ given by Eq. (25). The dependence of the normalized lateral spring force on the normalized side deflection from the initial state is shown in Fig. 4 for different values of κ. It is evident that the force-deflection relations are similar to those of a shallow arch subjected to midpoint loading (e.g., Gjelsvik and Bodner[17]). In particular, it can be observed that for decreasing values of κ (decreasing values of β) the peak value of lateral force (the snap through point) and the lateral deflection at which this peak occurs both decrease. The symbols in Fig. 4 are correlated with the peak buckling loads shown in Fig. 5. These results indicate that for the thickest shell (Fig. 4a) the buckling load occurs well below the snap through point of the lateral load for the small geometric imperfection $\theta_0 = 1$ deg, but it occurs near the snap through point for $\theta_0 = 2$ deg. However, as the shell gets thinner the buckling load is controlled by the snap through point in the lateral spring. This implies that the buckling of the cylindrical shell is caused by localized buckling caused by shallow arch-like response.

Figure 5 shows the dependence of the normalized applied load P [Eq. (22a)] on the normalized axial deflection Δ [Eq. (22c)] for different values of the geometric imperfection θ_0 at the particular values of κ considered in Fig. 4. Of interest is that the postbifurcation behavior of the geometrically perfect model ($\theta_0 = 0$) is similar to that obtained by large deformation analyses of the axially compressed shell. Also noticeable from Fig. 5 is that the peak loads of the imperfect model are significantly reduced relative to the bifurcation load $P_s/P_c = 1$. The sensitivity to imperfections is relatively low for large values of κ (Fig. 5a) and is relatively high for small values of κ (Fig. 5d). Consequently, from the functional form $\beta(\kappa)$ shown in Fig. 2, it follows from Fig. 5 that the spring (structural) parameter $\beta(\kappa)$ significantly influences imperfection sensitivity of the model and of the related shell. This is shown directly in Figs. 6a and 6b, where the reduction of the buckling load parameter P_s/P_c is

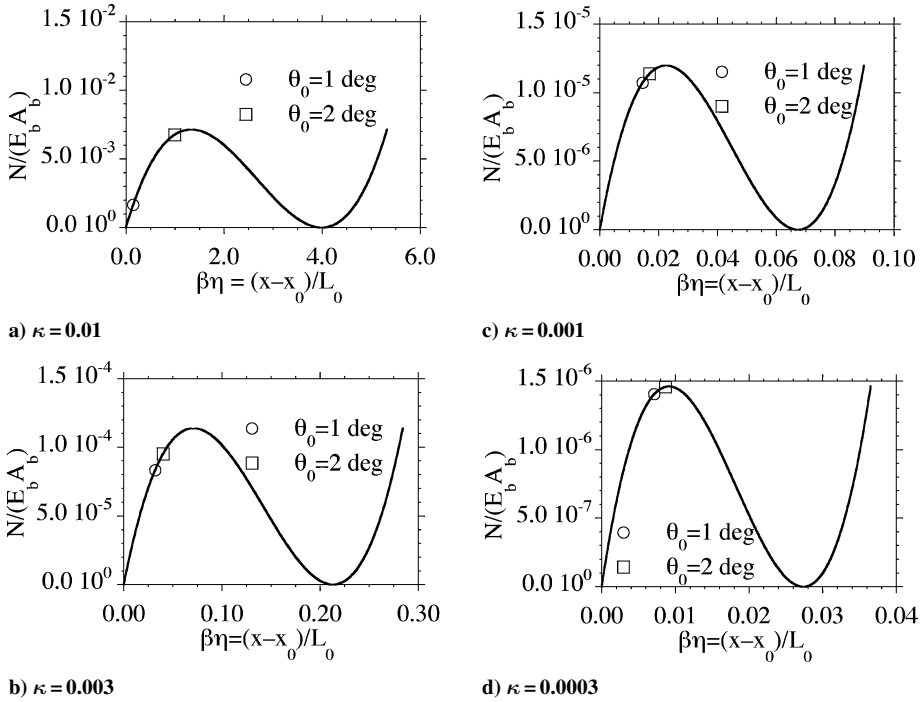

Fig. 4 Normalized load in the lateral spring of the model vs the normalized lateral deflection $\beta\eta$ for different values of κ. Note the changes in scale. The symbols are correlated with the peak loads in Fig. 5.

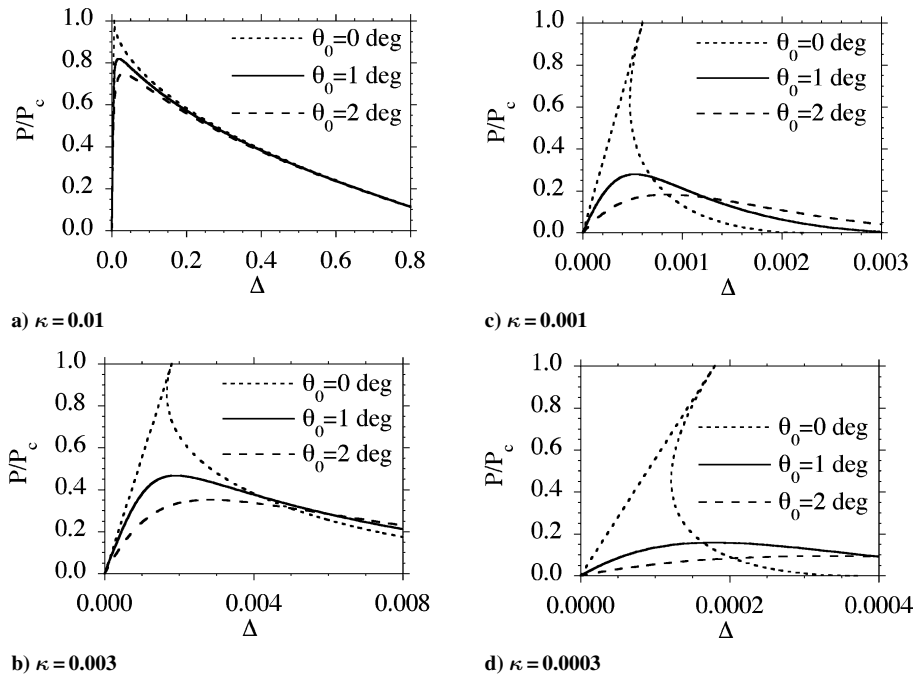

Fig. 5 Normalized axial load in the model vs normalized axial deflection Δ for different values of the imperfection angle θ_0 and different values of κ with variable $\beta(\kappa)$.

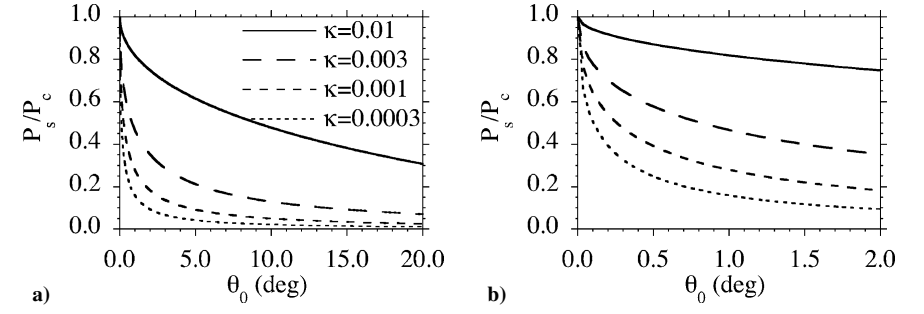

Fig. 6 Dependence of the normalized buckling (peak) load P_s/P_c on the imperfection angle θ_0 for different values of κ.

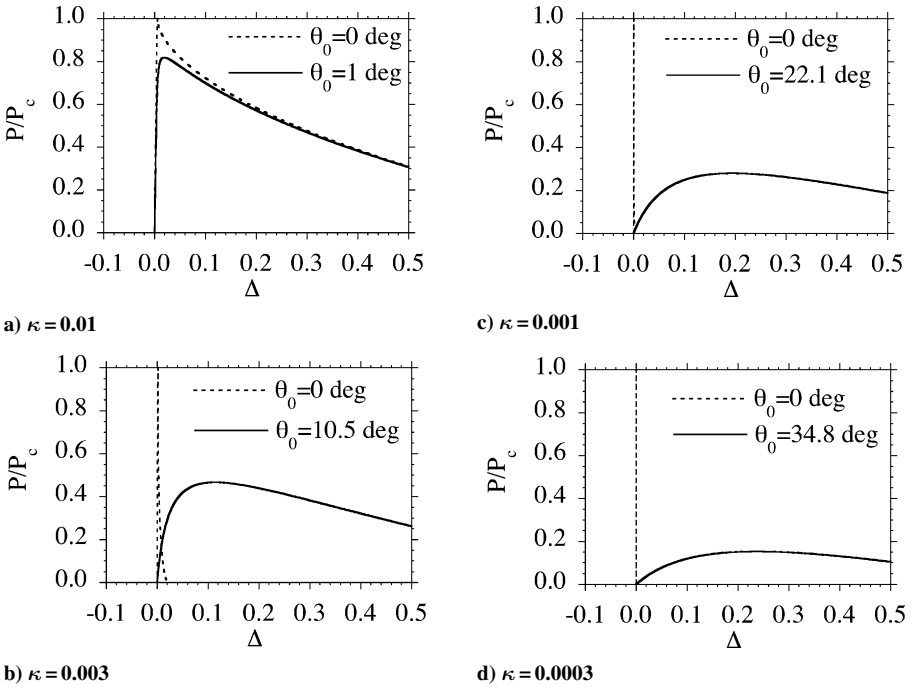

Fig. 7 Normalized axial load in the model vs normalized axial deflection Δ for different values of the imperfection angle θ_0 and different values of κ with constant $\beta = 1.331$.

calculated [with $\beta = \beta(\kappa)$ in Eq. (25)] as a function of the imperfection θ_0 for different values of κ.

Correlation Based on the Geometrical Parameter θ_0

Koiter's approximate formula (27) for axially compressed isotropic elastic shells implies that geometric imperfections are the main influence on the buckling (peak) load. This conjecture can also be explored within the context of the present model by specifying a constant value of the spring (structural) parameter β and adjusting the value θ_0 of the geometric imperfection for the model to match the empirical information (24). Specifically, β is taken to have the value predicted by the function form (25) for $\kappa = 0.01$:

$$\beta = 1.331 \tag{30}$$

Instead of proposing a form for θ_0 as a function of κ, the values of θ_0 required for values of P_s/P_c associated with the nonlinear model to enforce the correlation (24) of the shell were determined for only the four values of κ considered in Figs. 4 and 5. It can be seen from Fig. 7 that the results of these calculations lead to unphysically large values for the geometric imperfection θ_0. This emphasizes the importance of shell geometry $\kappa = t/R$ and accurate thickness measurements[18] on the buckling of axially loaded imperfect shells.

Conclusions

Given an accurate characterization of the imperfect geometry and boundary and loading conditions of a specific shell, it should be possible to predict the buckling (peak) load from a numerical solution of the complete nonlinear equations as described, for example, by Arbocz and Starnes.[1] However, such a numerical analysis does not by itself yield physical insight into the buckling process and the important features of the geometric imperfections.

Although lacking predictive capability, the simple mechanical model developed here demonstrates features that seem to be consistent with test observations on actual shells and can serve as a guide for further investigations. These include the following:

1) For correlating the model response with the buckling behavior of actual shells, it appears that both a representative parameter of the shell structure and a geometric imperfection parameter are necessary. In particular, it is found that determining the lateral spring characteristic of the model β in terms of the basic shell geometry $\kappa(=t/R)$ [based on Calladine's empirical formula (6) in the present exercise] leads to good agreement with details of the shell buckling behavior. In contrast, Koiter's approximate equation (1) for buckling of imperfect axially compressed shells considers only a geometric imperfection parameter.

2) Once the basic correlations between model and shell are made [Eqs. (23) and (24)], the model exhibits load deflection behavior (Fig. 5) and imperfection sensitivity (Fig. 6) similar to that of the shell. The latter is significantly enhanced for thin shells (small κ) relative to that for thick shells. These results imply that shell buckling under axial compressive loading can be viewed as a local event governed by shallow arch-like behavior where the extent of the arch depends on the shell geometry (κ). They also indicate that the specific geometry of local axial imperfections of the shell (out of straightness) might be more important than that of circumferential imperfections (out of roundness) for shell buckling under axial loading.

3) Attempts to match the empirical data for the buckling (peak) load by adjusting the value of the geometric imperfection θ_0 for different values of κ, holding the spring (structural) parameter β constant, lead to unphysically large values of the geometric imperfection. These results emphasize the importance of the dependence of the spring (structural) parameter β on κ. Moreover, they suggest that the buckling load of a cylindrical shell should also depend on a structural parameter in addition to a geometric imperfection.

4) The geometric imperfection θ_0 in the model cannot distinguish between displacement imperfections and slope imperfections. However, use of an imperfection slope factor rather than an imperfection displacement term might be more suitable for actual shells in some cases, such as the examination of the influence of local dents in the structure.

5) Except for large values of κ, the buckling (peak) load in the model occurs when the lateral spring force is close to the snap-through condition leading to a large deformation equilibrium state. This is consistent with observations of shells, which indicate that the mode of local initial buckling differs from that of the snap-through diamond shaped pattern into which the shell eventually deforms.

Finally, the results of the simple model considered in this paper suggest that future experiments and numerical calculations of buckling of cylindrical shells should pay more attention to mechanical aspects of the initial deformation and snap-through phenomena

occurring in localized buckling of the shell. That is, it might be useful to consider buckling as a local instability problem with the boundaries determined as part of the solution. This calls for detailed examination of the localized imperfections and the deformation modes from the onset of loading. In this regard, it is tempting to try to associate the geometry of the model, for example, the length L_0 of the bars, to the dimensions of the diamond-shaped buckle, but such a relation is speculative. Also, attention needs to be given to manufacturing variabilities. In particular, the recent work of Rubin[18] on the buckling of shallow arches emphasizes the importance of accurate measurements of the thickness of the shell because even standard tolerances can lead to thickness variations that cause significant reduction in peak load. For example, the tolerances for 3/16-in. aluminum plate allow a minimum thickness of $t = 4.41$ mm relative to the nominal thickness $t = 4.76$ mm. It then follows from Eqs. (23) and (24) that this minimum thickness would lead to a reduction of 11% in the nominal peak stress σ_s. Some studies on the influence of thickness imperfections are reported in Singer, et al.[2]

Appendix: Expression for the Peak Load

The objective of this Appendix is to develop an approximate expression for the peak load P_s in the model sketched in Fig. 1. In addition, an analytical expression for the function $\beta(\kappa)$ that causes the model to approximate the correlation (24) is developed. To this end, Eq. (20) is substituted into Eq. (22a) to deduce that

$$\frac{P}{E_bA_b} = \left\{ \frac{(\beta/9)[\alpha/(E_bA_b)](\eta^2 - 6\eta + 9)\eta}{\sin(\theta_0) + \beta\eta + (\beta/9)[\alpha/(E_bA_b)](\eta^2 - 6\eta + 9)\eta} \right\} \cos\theta \tag{A1}$$

Next, this equation is approximated by the form

$$\frac{P}{\alpha\beta} = \frac{\left(1 - \frac{2}{3}\eta\right)\eta\cos(\theta_0)}{\sin(\theta_0) + [1 + \alpha/(E_bA_b)]\beta\eta} \tag{A2}$$

Consequently, the peak load P_s associated with this approximate form occurs when the slope vanishes:

$$\frac{1}{\alpha\beta\cos(\theta_0)}\frac{\mathrm{d}P}{\mathrm{d}\eta}(\eta_s) = \left\{ \left[\sin(\theta_0) + \left(1 + \frac{\alpha}{E_bA_b}\right)\beta\eta_s \right] \times \left(1 - \frac{4}{3}\eta_s\right) - \left(1 - \frac{2}{3}\eta_s\right)\beta\eta_s\left(1 + \frac{\alpha}{E_bA_b}\right) \right\} \Big/ \left\{ \left[\sin(\theta_0) + \left(1 + \frac{P_c}{E_bA_b}\right)\beta\eta_s \right]^2 \right\} = 0 \tag{A3}$$

and η equals the value η_s given by

$$\eta_s = [\sin(\theta_0)/\beta][1 - P_c/(E_bA_b)](-1 + D)$$

$$D = \sqrt{1 + \tfrac{3}{2}[\beta/\sin(\theta_0)]/[1 - P_c/(E_bA_b)]} \tag{A4}$$

where use has been made of the expression (17). Thus, the peak load can be approximated by

$$P_s/P_c = (1 - 1/D)\left\{1 - \tfrac{2}{3}[\sin(\theta_0)/\beta] \times [1 - P_c/(E_bA_b)](D - 1)\right\}\cos(\theta_0) \tag{A5}$$

Next, Eq. (A5) is solved for the auxiliary quantity

$$\gamma = \sin(\theta_0)/\beta \tag{A6}$$

To this end, Eq. (A5) is multiplied by D, the result is expanded, and use is made of Eq. (A4) to replace the expression for D^2. The resulting equation can be solved for D and then squared to obtain a quadratic equation for γ of the form

$$a_2\gamma^2 + a_1\gamma - a_0 = 0 \tag{A7}$$

where the coefficients are given by

$$a_0 = \tfrac{3}{2}\{1 - P_s/[\cos(\theta_0)P_c]\}^2/[1 - P_c/(E_bA_b)] \tag{A8a}$$

$$a_1 = 4 - 4\{1 - P_s/[\cos(\theta_0)P_c]\} - \{1 - P_s/[\cos(\theta_0)P_c]\}^2 \tag{A8b}$$

$$a_2 = \tfrac{8}{3}\{P_s/[\cos(\theta_0)P_c]\}[1 - P_c/(E_bA_b)] \tag{A8c}$$

To make connection with Koiter's equation (1), Eq. (A7) can be further approximated for small values of θ_0 and (θ_0/β) by neglecting a_2 to obtain Eq. (8).

Returning to the general solution, the full equation (A7) can be solved for β to deduce

$$\beta = \hat{\beta}\left(\frac{P_c}{E_bA_b}, \frac{P_s}{P_c}, \theta_0\right) = \frac{\sin(\theta_0)}{\gamma}$$

$$\gamma = \frac{-a_1 + \sqrt{a_1^2 + 4a_2a_0}}{2a_2} \tag{A9}$$

Here, the spring (structural) parameter β is specified as a function of κ by fixing the value of the geometric imperfection θ_0 and using the correlations (23) for $P_c/(E_bA_b)$ and (24) for P_s/P_c, such that (for $\nu = 0.3$) Eq. (A9) yields Eq. (25).

Acknowledgments

The research of M. B. Rubin was partially supported by the fund for the promotion of research at the Technion. Also, the authors acknowledge helpful discussions with J. Singer and T. Weller.

References

[1]Arbocz, J., and Starnes, J. E., "On a High-Fidelity Hierarchical Approach to Buckling Load Calculations," *New Approaches to Structural Mechanics, Shells and Biological Structures*, edited by H. R. Drew and S. Pellegrino, Vol. 104, Solid Mechanics and Its Applications, Kluwer Academic, 2002, pp. 271–292.

[2]Singer, J., Abramovich, H., and Weller, T., "The Prerequisites for an Advanced Design Methodology in Shells Prone to Buckling," *New Approaches to Structural Mechanics, Shells and Biological Structures*, edited by H. R. Drew and S. Pellegrino, Vol. 104, Solid Mechanics and Its Applications, Kluwer Academic, 2002, pp. 393–411.

[3]Singer, J., Arbocz, J., and Weller, T., *Buckling Experiments: Experimental Methods in Buckling of Thin-Walled Structures*, Vol. 1, Wiley, New York, 1998.

[4]Singer, J., Arbocz, J., and Weller, T., *Buckling Experiments: Experimental Methods in Buckling of Thin-Walled Structures*, Vol. 2, Wiley, New York, 2002.

[5]Friedrichs, K. O., "On the Minimum Buckling Load for Spherical Shells," *Applied Mechanics*, Theodore von Kármán Anniversary Volume, California Inst. of Technology, Pasadena, CA, 1941, pp. 258–272.

[6]Koiter, W. T., "Over de Stabiliteit van het Elastisch Evenwicht (On the Stability of Elastic Equilibrium)," Ph.D. Dissertation, Delft, The Netherlands, 1945 (English translation issued as NASA TT F-10, 833, 1967).

[7]Hutchinson, J. W., and Koiter, W. T., "Postbuckling Theory," *Applied Mechanical Reviews*, Vol. 23, 1970, pp. 1353–1363.

[8]Timoshenko, S. P., and Gere, J. M., *Theory of Elastic Stability*, McGraw–Hill, New York, 1961, Sec. 11.1.

[9]Budiansky, B., and Hutchinson, J. W., "Dynamic Buckling of Imperfection-Sensitive Structures," *Proceedings of the XI International Congress of Applied Mechanics*, edited by H. Gortler, Springer-Verlag, Berlin, 1966, pp. 636–651.

[10]Budiansky, B., "Dynamic Buckling of Elastic Structures: Criteria and Estimates," *Proceedings of an International Conference on Dynamic Stability of Structures*, edited by G. Herrmann, Pergamon, Oxford, 1965, pp. 83–106.

[11]Hutchinson, J. W., and Budiansky, B., "Dynamic Buckling Estimates," *AIAA Journal*, Vol. 4, No. 3, 1966, pp. 525–530.

[12]Kounadis, A. N., Raftoyiannis, J., and Mallis, J., "Dynamic Buckling of an Arch Model Under Impact Loading," *Journal of Sound and Vibration*, Vol. 134, No. 2, 1989, pp. 193–202.

[13]von Kármán, T., Dunn, L. G., and Tsien, H., "The Influence of Curvature on the Buckling Characteristics of Structures," *Journal of the Aeronautical Sciences*, Vol. 7, No. 7, 1940, pp. 276–289.

[14]Calladine, C. R., "A Shell-Buckling Paradox Resolved," *Advances in the Mechanics of Plates and Shells*, edited by D. Durban, D. Givoli, and J. G. Simonds, Kluwer Academic, Norwell, MA, 2001, pp. 119–134.

[15]Hoff, N. J., 'Some Recent Studies on the Buckling of Thin Shells," *Aeronautical Journal of the Royal Aeronautical Society*, Vol. 73, 1969, pp. 1057–1070.

[16]Weingarten, V. I., Morgan, E. J., and Seide, P., "Elastic Stability of Thin-Walled Cylindrical and Conical Shells Under Axial Compression," *AIAA Journal*, Vol. 3, No. 3, 1965, pp. 500–505.

[17]Gjelsvik, A., and Bodner, S. R., "The Energy Criterion and Snap Buckling of Arches," *Journal of the Engineering Mechanics Division, ASCE*, Vol. 88, 1962, pp. 87–134.

[18]Rubin, M. B., "Buckling of Elastic Shallow Arches Using the Theory of a Cosserat Point," *Journal of Engineering Mechanics*, Vol. 130, 2004, pp. 216–224.

A. Palazotto
Associate Editor